*Sandeep Kumar Paul, Manoj Sahni*

# TWO-DIMENSIONAL STRESS ANALYSIS OF A THICK HOLLOW CYLINDER MADE OF FUNCTIONALLY GRADED MATERIAL SUBJECTED TO NON-AXISYMMETRIC LOADING

# DVODIMENZIONALNA ANALIZA NAPONA DEBELOZIDOG ŠUPLJEG CILINDRA OD FUNKCIONALNOG MATERIJALA OPTEREĆEN NEOSNOSIMETRIČNO

Originalni naučni rad / Original scientific paper
UDK /UDC:

Rad primljen / Paper received: 6.04.2021

Adresa autora / Author's address:
Department of Mathematics, PDPU, Gandhinagar, India
email: sandeeppaulkumar@gmail.com,
manojsahani117@gmail.com

**Keywords**
- functionally graded material
- cylinder
- Young's modulus
- pressure
- stresses

*Abstract*

*In this study, a thick hollow functionally graded cylinder is considered for the analysis of two-dimensional steady state mechanical stress in radial and circumferential directions under non-axisymmetric loading. Young's modulus is differing with continuous nonlinear variation in the thickness direction, and Poisson's ratio is invariant. Fourier half range series and Euler differential equations are considered as methods of analysis. Mechanical boundary conditions are implemented at internal and external surfaces of the cylinder and the graphs are plotted for derived results. This study may be useful in the application of pressure vessels.*

**Ključne reči**
- funkcionalni materijal
- cilindar
- Jangov modul elastičnosti
- pritisak
- naponi

*Izvod*

*U ovom radu se analizira dvodimenzionalno stacionarno mehaničko naponsko stanje u radijalnom i obimskom pravcu pri neosnosimetričnom opterećenju debelozidog šupljeg cilindra od funkcionalnog materijala. Jangov modul elastičnosti se menja kontinualno nelinearno u pravcu debljine, a Poasonov koeficijent je nepromenljiv. Furijeov red na poluintervalu i Ojlerove diferencijalne jednačine se koriste za metode analize. Mehanički granični uslovi su definisani za unutrašnju i spoljašnju površinu cilindra, a dobijeni rezultati su prikazani dijagramski. Ova analiza može biti korisna za primenu kod posuda pod pritiskom.*

## INTRODUCTION

Materials play a very important role in the evolution of human civilization. In the early stages of civilization, humans have associated ages with them such as Stone age, Bronze age, etc. Materials are being developed depending on the requirement and its usage and have been classified depending on their properties. Composite materials, also called space age materials, are used at various places, such as in aerospace, military equipment, medical field, pressure vessels, etc. A serious drawback of delamination which is also a major cause of failure of components has led to the birth of a new different class of materials called functionally graded materials (FGMs). FGM are such materials that can withstand high temperature and are equally good in strength as compared to composite materials. But by the lapse of time, engineers and researchers have applied the idea of FGM in several structural problems. They have worked on the stress management at interface level of the composite material to reduce stress concentration. Usually, FGMs are used in the design of several mechanical and thermal components to optimise the thermomechanical response of structures under thermal and mechanical loading. Basically, FGMs are non-homogeneous engineering materials in which the microstructure varies incessantly from one material to another /1/. Engineers can design multipurpose devices due to optimised control of thermomechanical properties of the material in different directions, /2/.

In recent years, many researchers have worked on thermo-mechanical stresses for functionally graded sphere and cylinder along radial direction only. But there are a smaller number of researchers who are working on FGM as 2-D and 3-D thermomechanical problems under steady and unsteady state conditions due to axisymmetric and non-axisymmetric loading. A long hollow cylinder of functionally graded material is analysed under inner pressure and uniform heat generation by Evci and Gülgeç, /3/. Jabbari et al. /4/ have examined a functionally graded cylinder for the thermomechanical response, subjected to non-axisymmetric loading under steady-state condition. They have applied complex Fourier series method to solve the governing equations of stress and displacement. An axisymmetric 2-D problem for finite thick hollow cylinder is considered for the analysis of wave propagation using finite element method (FEM) under effective internal pressure, /5/. Elastic and plastic stresses under external and internal pressures are evaluated for thick-walled spherical pressure vessel having FGM coating at inner surface, /6/. A study of creep stresses for rotating composite cylinder of $SiC_p$ is done by Sahni et. al. /7/, in which material gradation is varying exponentially over the volume. Sahni et. al. /8-9/ considered a cylinder with variation in thickness and a rotating disc in the analysis of stresses in the radial direction. Paul and Sahni /10/ have applied power series method to get analytical results for 2-D stresses of an axisymmetric FGM cylindrical pressure

vessel under steady state condition. Stress analysis of a rotating disc along its radial direction is examined by Singh et al. /11/. A functionally graded thick hollow spherical vessel and an infinite cylindrical vessel are investigated analytically for thermal stress along radial direction under the steady-state condition by Yıldırım, /12/. They have used the theory of one-dimensional Fourier heat conduction along with Dirichlet's boundary conditions and Cauchy-Euler differential equation for the problem. An FGM hollow cylinder having an elliptic hole is examined for thermomechanical response under thermal and mechanical loadings as a plane strain problem by Fesharaki et al. /13/. Material properties are differing by power law function in the elliptic cylindrical direction with fixed Poisson's ratio. Delouei et al. /14/ obtained a direct solution for the functionally graded (FG) cylindrical sector under steady-state heat conduction using Fourier theory. Power law function is used for the variation of material properties in radial and circumferential direction. A right circular cylinder made of functionally graded material is analysed for the behaviour of nonlinear vibration due to thermal environment having non-uniform mechanical loading along the corners and harmonic force in radial direction. Material properties of the simply supported shell are temperature dependent and considered to vary in the radial dimension as power-law function and its analysis is done by Yadav et al. /15/. Sofiyev et al. /16/ have solved a buckling problem for shells of FGM by applying mixed boundary conditions under uniform compressive lateral pressure. In this FGM model, the differential equations are developed for FGM shells using classical shell theory (CST). Shao et al. /17/ have considered an FGM as molybdenum/mullite that follow exponential law along radial coordinate.

Jabbari et. al. /18/ have utilized multi-layer method and theory of higher order shear deformation for the semi-analytical inspection of thermoelastic response for a thick rotating cylindrical pressure vessel consisted of functionally graded material with varying thickness under temperature gradient and non-uniform inner pressure loading. Displacement and stresses are examined under the influence of thermal variation and material gradation parameter with different geometries of the disk by Bayat et al. /19/. Using infinitesimal theory of elasticity and power series method, an isotropic FG cylindrical pressure vessel is examined for stresses and displacements subjected to internal pressure. Exponential function is assumed for the variation of Young's modulus along the thickness direction and Poisson's ratio is invariant /20/. An orthotropic functionally graded panel with fibre reinforcement is investigated for three-dimensional stresses under steady state condition using differential quadrature method, /21/. Kayhani et. al has derived analytical solution for heat conduction problem in the laminated composite cylinder using the Sturm-Liouville theorem /24/. Kamdi and Lamba /25/ have obtained an analytical solution for an inverse thermoelastic problem of isotropic hollow cylinder having finite length which is made of functionally graded material. For numerical calculations, the authors have considered an FGM cylinder made of ceramic-metal ($Al_2O_3$-Ni) with varying metallic component. Using plate theory of first order shear deformation, the solution of Navier equation is derived for free vibration and static bending analysis of a simply supported FG plate under the effect of porous medium, /26/. Le et. al /27/ have estimated the response of nonlinear buckling of a laminated composite cylindrical shell consisting of functionally graded graphene-reinforcement due to axial compressive load that is bounded by Pasternak's elastic foundation in a thermal environment. Numerical evaluation is done for the effects of geometrical properties, environment temperature, foundation, and graphene distribution on buckling response of the shell. An axisymmetric functionally graded cylinder is investigated for thermal stress with thermal conductivity that changes in radial and longitudinal directions by following a power law /28/. Under the effect of high temperatures and temperature differences a FGM thick hollow cylinder and sphere are explored for the analysis of nonlinear thermal stress by Yarimpabuç, /29/. Material properties are depending on temperature and radial gradation, but Poisson's ratio is considered invariant. The Fourier half range series is used in solving the governing differential equations under non-axisymmetric mechanical loading. A thick-walled tube formed of FGM is considered for the inspection of thermo-elastic response due to mechanical load under steady state condition, /30/. By applying uniaxial and biaxial loading on an FGM plate with elliptic hole, prediction is made for stress concentration factors using the finite element method, /31/.

In this study, the modulus of elasticity is assumed with nonlinear variation in thickness direction but Poisson's ratio is fixed and remains invariant. Displacements, strains, and stresses are investigated in the radial and circumferential directions under steady state condition due to non-axisymmetric mechanical loading. Fourier half range series and Euler differential equations are used to solve the Navier equations. Stresses are obtained by applying mechanical boundary conditions at inner and outer surfaces of the cylinder. Boundary conditions are varying along tangential direction and graphs are plotted for the numerical results of displacements and stresses in this problem.

## PROBLEM DESCRIPTION

Consider a thick hollow functionally graded cylinder with internal '$r_1$' and external radius '$r_2$'. Cylindrical coordinate axes ($r,\theta,z$) are assumed for FGM cylinder that refer to radial length, polar angle, and axial length, in respect, with internal '$p_1(\theta)$' and external pressure '$p_2(\theta)$' as shown in Fig. 1.

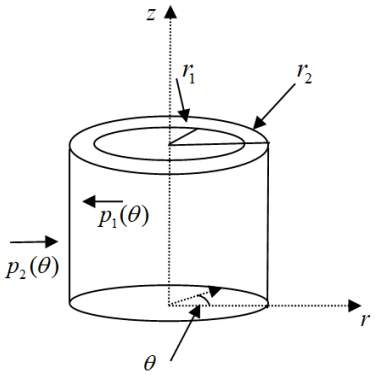


Figure 1. Thick hollow cylinder with cylindrical coordinates having pressures.

Stresses, strains and displacements vary along '$r$' and '$\theta$' dimensions. The modulus of elasticity has a smooth and continuous variation along the radial direction and follows the nonlinear form as

$$E(r)=E_0 r_2^{\alpha\log(r)}, \tag{1}$$

where: $E_0$ refers to Young's modulus, constant at $\alpha = 0$; and $\alpha$ is material gradation parameter.

The Hooke's law for functionally graded material can be written as, /22/,

$$\begin{aligned}\sigma_{rr}&=(\gamma+2\delta)\varepsilon_{rr}+\gamma\varepsilon_{\theta\theta},\\ \sigma_{\theta\theta}&=\gamma\varepsilon_{rr}+(\gamma+2\delta)\varepsilon_{\theta\theta},\\ \sigma_{r\theta}&=2\delta\varepsilon_{r\theta},\end{aligned} \tag{2}$$

where: $\sigma_{ij}$ and $\varepsilon_{ij}$ represent stress and strain tensors for $i, j = r, \theta$.

Lame's constants $\gamma$ and $\delta$, involving Young's modulus $E(r)$ and Poisson's ratio $\nu$ are written as, /22/,

$$\gamma=\frac{\nu E(r)}{(1+\nu)(1-2\nu)},\quad \delta=\frac{E(r)}{2(1+\nu)}. \tag{3}$$

Strain-displacement equations are assumed in the radial and circumferential directions as, /23/,

$$\varepsilon_{rr}=\frac{\partial u}{\partial r},\quad \varepsilon_{\theta\theta}=\frac{u}{r}+\frac{1}{r}\frac{\partial w}{\partial\theta},\quad \varepsilon_{r\theta}=\frac{1}{2}\left(\frac{1}{r}\frac{\partial u}{\partial\theta}+\frac{\partial w}{\partial r}-\frac{w}{r}\right), \tag{4}$$

where: $u$ and $w$ are components of radial and tangential displacements, respectively.

Stress equilibrium equations, ignoring inertia and body forces in radial and circumferential dimensions are, /4/,

$$\begin{aligned}&\frac{\partial\sigma_{rr}}{\partial r}+\frac{1}{r}\frac{\partial\sigma_{r\theta}}{\partial\theta}+\frac{1}{r}(\sigma_{rr}-\sigma_{\theta\theta})=0,\\ &\frac{\partial\sigma_{r\theta}}{\partial r}+\frac{1}{r}\frac{\partial\sigma_{\theta\theta}}{\partial\theta}+\frac{2}{r}\sigma_{r\theta}=0.\end{aligned} \tag{5}$$

Using Eqs.(1)-(5), the stress equations can be written in the form of displacements as

$$u_{rr}+(\alpha\log r_2+1)\frac{1}{r}u_r+\left(\frac{\nu\alpha\log r_2}{1-\nu}-1\right)\frac{u}{r^2}+\left(\frac{1-2\nu}{2-2\nu}\right)\frac{1}{r^2}u_{\theta\theta}+$$
$$+\frac{1}{2-2\nu}\frac{1}{r}w_{r\theta}+\left(\frac{(4+2\alpha\log r_2)\nu-3}{2-2\nu}\right)\frac{1}{r^2}w_\theta=0, \tag{6}$$

$$w_{rr}+(\alpha\log r_2+1)\frac{1}{r}w_r-(\alpha\log r_2+1)\frac{w}{r^2}+\left(\frac{2-2\nu}{1-2\nu}\right)\frac{1}{r^2}w_{\theta\theta}+$$
$$+\frac{1}{2-2\nu}\frac{1}{r}u_{r\theta}+\left(\frac{3-4\nu}{1-2\nu}+\alpha\log r_2\right)\frac{1}{r^2}u_\theta=0, \tag{7}$$

where: Eqs.(6) and (7) represent Navier equations in the form of second order partial differential equations.

Radial and tangential displacements are stated in the form of Fourier half range series as

$$u(r,\theta)=\sum_{k=0}^{\infty}U_k(r)\cos k\theta,\quad w(r,\theta)=\sum_{k=0}^{\infty}W_k(r)\sin k\theta, \tag{8}$$

where: $U_k(r)=\frac{1}{2\pi}\int_{-\pi}^{\pi}u(r,\theta)\cos k\theta d\theta$ and

$W_k(r)=\frac{1}{2\pi}\int_{-\pi}^{\pi}w(r,\theta)\sin k\theta d\theta$ are Fourier coefficients along the radius for different values of $k$.

Placing Eq.(8) into Eqs.(6) and (7), we get

$$U_k''(r)+(\alpha\log r_2+1)\frac{1}{r}U_k'(r)+\left(\frac{\nu\alpha\log r_2}{1-\nu}-1-k^2\frac{1-2\nu}{2-2\nu}\right)\frac{U_k(r)}{r^2}+$$
$$+\left(\frac{k}{2-2\nu}\right)\frac{1}{r}W_k'(r)+\left(\frac{(4+2\alpha\log r_2)\nu-3}{2-2\nu}\right)\frac{k}{r^2}W_k(r)=0, \tag{9}$$

$$W_k''(r)+(\alpha\log r_2+1)\frac{1}{r}W_k'(r)-\left(\alpha\log r_2+1+k^2\frac{2-2\nu}{1-2\nu}\right)\frac{W_k(r)}{r^2}-$$
$$-\left(\frac{k}{2-2\nu}\right)\frac{1}{r}U_k'(r)-\left(\frac{3-4\nu}{1-\nu}+\alpha\log r_2\right)\frac{k}{r^2}U_k(r)=0. \tag{10}$$

Equations (9) and (10) represent Euler ordinary differential equations whose general solution can be found by the method of substitution as

$$U_k(r)=Lr^\lambda,\quad W_k(r)=Mr^\lambda. \tag{11}$$

Substituting Eq. (11) into Eqs.(9) and (10), we get

$$\left[\lambda(\lambda-1)+(\alpha\log r_2+1)\lambda+\frac{\nu\alpha\log r_2}{1-\nu}-1-\frac{1-2\nu}{2-2\nu}k^2\right]L+$$
$$+k\left[\frac{\lambda}{2-2\nu}+\frac{(4+2\alpha\log r_2)\nu-3}{2-2\nu}\right]M=0, \tag{12a}$$

$$\left[\lambda(\lambda-1)+(\alpha\log r_2+1)\lambda-\alpha\log r_2-1-\frac{2-2\nu}{1-2\nu}k^2\right]M-$$
$$-k\left(\frac{\lambda}{1-2\nu}+\frac{3-4\nu}{1-2\nu}+\alpha\log r_2\right)L=0. \tag{12b}$$

Equations (12a) and (12b) give homogeneous system of linear equations in $L$ and $M$, so it can be written in the matrix form as

$$\begin{bmatrix}P_1 & P_2\\ P_3 & P_4\end{bmatrix}\begin{bmatrix}L\\ M\end{bmatrix}=\begin{bmatrix}0\\ 0\end{bmatrix}, \tag{13}$$

where:

$$P_1=\lambda(\lambda-1)+(\alpha\log r_2+1)\lambda+\frac{\nu\alpha\log r_2}{1-\nu}-1-\frac{1-2\nu}{2-2\nu}k^2;$$

$$P_2=k\left(\frac{\lambda}{2-2\nu}+\frac{(4+2\alpha\log r_2)\nu-3}{2-2\nu}\right);$$

$$P_3=-k\left(\frac{\lambda}{1-2\nu}+\frac{3-4\nu}{1-2\nu}+\alpha\log r_2\right);\ \text{and}$$

$$P_4=\lambda(\lambda-1)+(\alpha\log r_2+1)\lambda-\alpha\log r_2-1-\frac{2-2\nu}{1-2\nu}k^2.$$

To get the non-trivial solution for Eq.(12), taking $\det\begin{bmatrix}P_1 & P_2\\ P_3 & P_4\end{bmatrix}=0$, and hence

$$\left[\lambda(\lambda-1)+(\alpha\log r_2+1)\lambda+\frac{\nu\alpha\log r_2}{1-\nu}-1-\frac{1-2\nu}{2-2\nu}k^2\right]\times$$
$$\times\left[\lambda(\lambda-1)+(\alpha\log r_2+1)\lambda-\alpha\log r_2-1-\frac{2-2\nu}{1-2\nu}k^2\right]+k^2\times$$
$$\times\left(\frac{\lambda}{2-2\nu}+\frac{(4+2\alpha\log r_2)\nu-3}{2-2\nu}\right)\left(\frac{\lambda}{1-2\nu}+\frac{3-4\nu}{1-2\nu}+\alpha\log r_2\right)=0 \tag{14}$$

Solving Eq.(14) for $\lambda$, we get four eigen values $\lambda_{ki}$($i$ = 1, 2, 3, 4) for different $k$, and using these values, general solutions for Eq.(11) are obtained as

$$U_k(r)=\sum_{i=1}^{4}L_{ki}r^{\lambda_{ki}}\ ,\quad W_k(r)=\sum_{i=1}^{4}H_{ki}L_{ki}r^{\lambda_{ki}}\ , \qquad (15)$$

where: $H_{ki}$ represents the relation between $L_{ki}$ and $M_{ki}$, that can be obtained from Eq.(12a) as

$$H_{ki}=\frac{-\left(\lambda_{ki}(\lambda_{ki}-1)+(\alpha\log r_2+1)\lambda_{ki}+\frac{\nu\alpha\log r_2}{1-\nu}-1-\frac{1-2\nu}{2-2\nu}k^2\right)}{k\left(\frac{\lambda_{ki}}{2-2\nu}+\frac{(4+2\alpha\log r_2)\nu-3}{2-2\nu}\right)}$$

If we consider $k = 0$, then Eqs.(9) and (10) can be converted into two differential equations as

$$U_0''(r)+(\alpha\log r_2+1)\frac{1}{r}U_0'(r)+\frac{1}{r^2}\left(\frac{\nu}{1-\nu}\alpha\log r_2-1\right)U_0(r)=0 \qquad (16a)$$

$$W_0''(r)+(\alpha\log r_2+1)\frac{1}{r}W_0'(r)-(\alpha\log r_2+1)\frac{1}{r^2}W_0(r)=0\,. \qquad (16b)$$

Solving ordinary differential Eqs.(16a) and (16b), we get the general solution for $U_0(r)$ and $W_0(r)$ as

$$U_0(r)=\sum_{i=1}^{2}L_{0i}r^{\lambda_{0i}}\ ,\quad W_0(r)=\sum_{i=3}^{4}L_{0i}r^{\lambda_{0i}}\ , \qquad (17)$$

where:

$$\lambda_{01},\lambda_{02}=\frac{1}{2}\left[-\alpha\log r_2\mp\left((\alpha\log r_2)^2-4\left(\frac{\nu\alpha\log r_2}{1-\nu}-1\right)\right)^{1/2}\right];$$

$\lambda_{03}=-(\alpha\log r_2+1)$, and $\lambda_{04}=1$.

Thus, using Eqs.(8), (15) and (17), complete solutions of the displacements along radial and tangential directions for each $k$ are given as

$$\begin{aligned}u(r,\theta)&=\sum_{i=1}^{2}L_{0i}r^{\lambda_{0i}}+\sum_{k=1}^{\infty}\left[\sum_{i=1}^{4}L_{ki}r^{\lambda_{ki}}\right]\cos k\theta,\\ w(r,\theta)&=\sum_{k=1}^{\infty}\left[\sum_{i=1}^{4}H_{ki}L_{ki}r^{\lambda_{ki}}\right]\sin k\theta.\end{aligned} \qquad (18)$$

Using strain-displacements relation from Eq.(4) and stress equations from Eq.(5), we can find strains and stresses in radial and tangential directions as

$$\varepsilon_{rr}=\sum_{i=1}^{2}L_{0i}\lambda_{0i}r^{\lambda_{0i}-1}+\sum_{k=1}^{\infty}\left[\sum_{i=1}^{4}L_{ki}\lambda_{ki}r^{\lambda_{ki}-1}\right]\cos k\theta\,, \qquad (19a)$$

$$\varepsilon_{\theta\theta}=\sum_{i=1}^{2}L_{0i}r^{\lambda_{0i}-1}+\sum_{k=1}^{\infty}\left[\sum_{i=1}^{4}L_{ki}r^{\lambda_{ki}-1}\right]\cos k\theta+\sum_{k=1}^{\infty}\left[\sum_{i=1}^{4}kH_{ki}L_{ki}r^{\lambda_{ki}-1}\right]\cos k\theta\,, \qquad (19b)$$

$$\varepsilon_{r\theta}=\frac{1}{2}\left(-\sum_{k=1}^{\infty}\left[\sum_{i=1}^{4}kL_{ki}r^{\lambda_{ki}-1}\right]\sin k\theta+\sum_{k=1}^{\infty}\left[\sum_{i=1}^{4}H_{ki}L_{ki}(\lambda_{ki}-1)r^{\lambda_{ki}-1}\right]\sin k\theta\right), \qquad (19c)$$

$$\sigma_{rr}=\frac{(1-\nu)E(r)}{(1+\nu)(1-2\nu)}\left(\sum_{i=1}^{2}L_{0i}\lambda_{0i}r^{\lambda_{0i}-1}+\sum_{k=1}^{\infty}\left[\sum_{i=1}^{4}L_{ki}\lambda_{ki}r^{\lambda_{ki}-1}\right]\cos k\theta\right)+$$
$$+\frac{\nu E(r)}{(1+\nu)(1-2\nu)}\left(\sum_{i=1}^{2}L_{0i}r^{\lambda_{0i}-1}+\sum_{k=1}^{\infty}\left[\sum_{i=1}^{4}L_{ki}r^{\lambda_{ki}-1}\right]\cos k\theta+\sum_{k=1}^{\infty}\left[\sum_{i=1}^{4}kH_{ki}L_{ki}r^{\lambda_{ki}-1}\right]\cos k\theta\right), \qquad (20a)$$

$$\sigma_{\theta\theta}=\frac{(1-\nu)E(r)}{(1+\nu)(1-2\nu)}\left(\sum_{i=1}^{2}L_{0i}r^{\lambda_{0i}-1}+\sum_{k=1}^{\infty}\left[\sum_{i=1}^{4}L_{ki}r^{\lambda_{ki}-1}\right]\cos k\theta+\right.$$
$$\left.+\sum_{k=1}^{\infty}\left[\sum_{i=1}^{4}kH_{ki}L_{ki}r^{\lambda_{ki}-1}\right]\cos k\theta\right)+\frac{\nu E(r)}{(1+\nu)(1-2\nu)}\times$$
$$\times\left(\sum_{i=1}^{2}L_{0i}\lambda_{0i}r^{\lambda_{0i}-1}+\sum_{k=1}^{\infty}\left[\sum_{i=1}^{4}L_{ki}\lambda_{ki}r^{\lambda_{ki}-1}\right]\cos k\theta\right), \qquad (20b)$$

$$\sigma_{r\theta}=\frac{1}{2}\frac{E(r)}{(1+\nu)}\left(-\sum_{k=1}^{\infty}\left[\sum_{i=1}^{4}kL_{ki}r^{\lambda_{ki}-1}\right]\sin k\theta+\right.$$
$$\left.+\sum_{k=1}^{\infty}\left[\sum_{i=1}^{4}H_{ki}L_{ki}(\lambda_{ki}-1)r^{\lambda_{ki}-1}\right]\sin k\theta\right). \qquad (20c)$$

In Eqs.(18), (19a)-(19c), and (20a)-(20c), four unknowns $L_{ki}(i = 1,2,3,4)$ can be evaluated by applying any four boundary conditions picked from the following general mechanical boundary conditions as

$$\begin{aligned}u(r_1,\theta)&=f_1(\theta),\quad u(r_2,\theta)=f_2(\theta)\\ w(r_1,\theta)&=f_3(\theta),\quad w(r_2,\theta)=f_4(\theta)\\ \sigma_{rr}(r_1,\theta)&=f_5(\theta),\quad \sigma_{rr}(r_2,\theta)=f_6(\theta)\\ \sigma_{r\theta}(r_1,\theta)&=f_7(\theta),\quad \sigma_{r\theta}(r_2,\theta)=f_8(\theta)\end{aligned} \qquad (21)$$

where: $f_j(\theta)$ $(j = 1,2,\ldots,8)$ are some known functions of $\theta$ on inner and outer surfaces of the cylinder.

## NUMERICAL RESULTS

Consider inner and outer radii respectively as $r_1 = 1.2$, $r_2 = 1.4$ in metres. Poisson ratio $\nu = 0.3$ and constant Young's modulus $E_0 = 200$ GPa for a thick hollow FGM cylinder, and mechanical boundary conditions are defined as

$$\begin{aligned}&\sigma_{rr}(r_1,\theta)=50+150\cos 2\theta+200\cos 3\theta\ \text{ MPa}\\ &\sigma_{r\theta}(r_1,\theta)=50\sin 2\theta\ \text{ MPa}\\ &u(r_2,\theta)=0,\quad w(r_2,\theta)=0,\end{aligned} \qquad (22)$$

where: radial and shear stresses are varying along the circumferential direction at inner radius, and there is no radial and tangential displacement along $\theta$ direction at outer radius.

Figures 2-6 represent displacements and stresses in the radial and tangential directions at $\alpha = 1$.

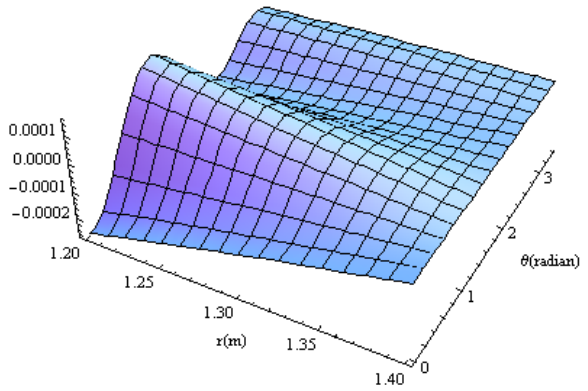


Figure 2. Radial displacement, $u$ (m), at $\alpha = 1$.

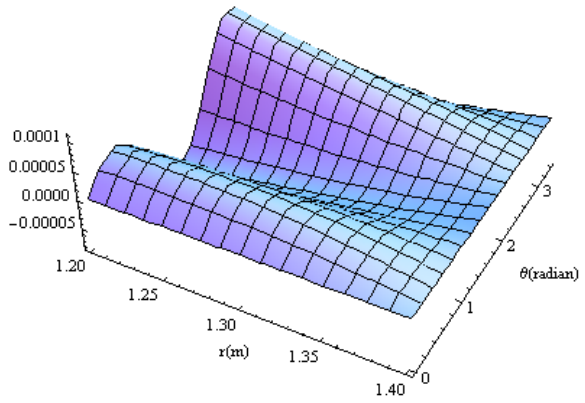


Figure 3. Circumferential displacement, $w$ (m), at $\alpha = 1$.

In Figs. 2 and 3, radial and circumferential displacements are presented respectively. Circumferential displacement is less than the radial displacement. Both displacements are zero at outer radius through the radians, and hence, assure the completeness of boundary conditions.

Figures 4 to 6 represent radial, circumferential, and shear stresses along radial and tangential direction. Radial stresses are higher than hoop and shear stresses in magnitude. On the other side, shear stresses are lower than radial and hoop stresses. In Fig. 4, radial stresses are decreasing in magnitude near zero radian, but increasing in magnitude for 3.14 radian as thickness varies from inner to outer radius. Figure 6 shows that shear stress remains constant, i.e. zero for zero radian, but continuously decreases for each radial value as it varies from inner to outer radii.

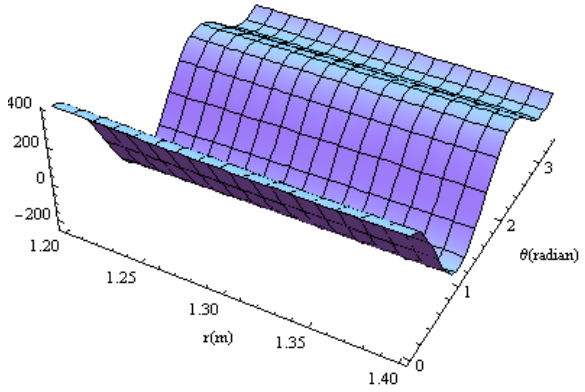


Figure 4. Radial stress, $\sigma_{rr}$ (MPa), at $\alpha = 1$.

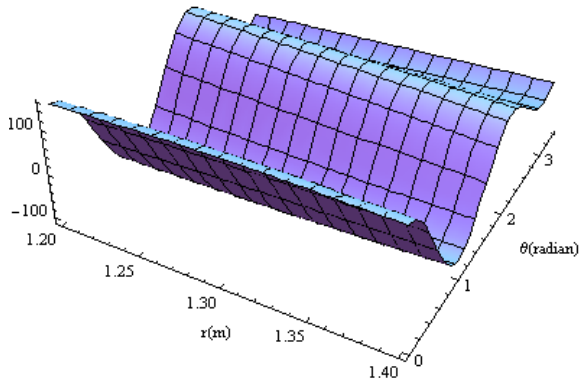


Figure 5. Circumferential stress, $\sigma_{\theta\theta}$ (MPa), at $\alpha = 1$.

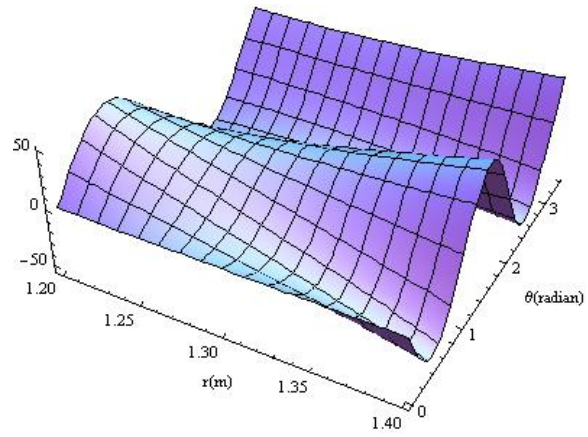


Figure 6. Shear stress, $\sigma_{r\theta}$ (MPa), at $\alpha = 1$.

Figures 7-9 represent mechanical stresses for different random values of gradation parameter $\alpha = 0,1,3,5,7$ at $\theta = \pi/4$. Variations in mechanical stresses can be seen along radial direction for particular $\theta = \pi/4$. The material is homogenous for $\alpha = 0$.

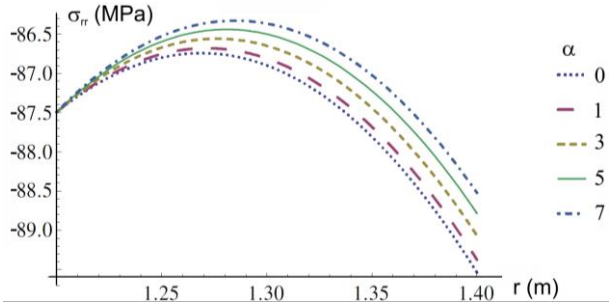


Figure 7. Radial stresses at $\theta = \pi/4$ for different values of material parameter $\alpha = 0,1,3,5,7$.

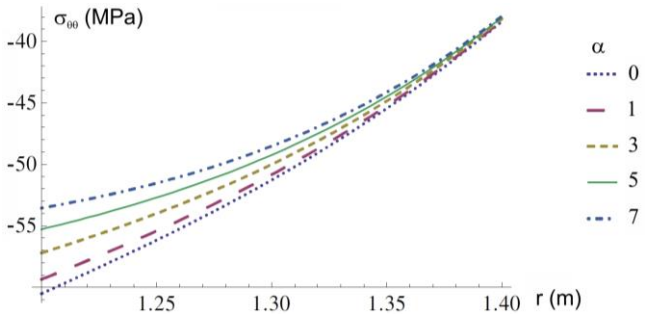


Figure 8. Circumferential stresses at $\theta = \pi/4$ for different values of material parameter $\alpha = 0.1.3.5.7$.

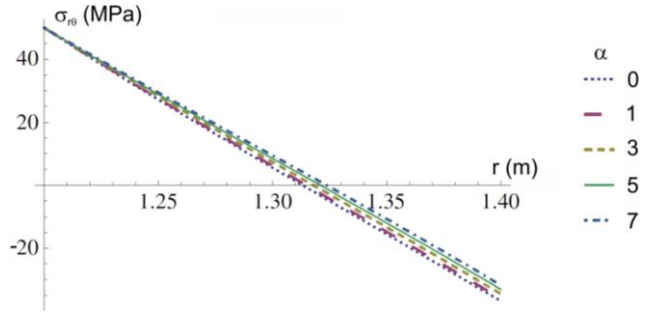


Figure 9. Shear stresses at $\theta = \pi/4$ for different values of material parameter $\alpha = 0,1,3,5,7$.

In Figs. 7 and 8, as gradation parameter increases from 0 to 7, Young's modulus also increases, but radial and hoop stresses decrease in magnitude along inner to outer radius at $\theta = \pi/4$. On the other hand, shear stresses are increasing in magnitude as gradation index parameter increases along the radial travel from inner to outer at the radian $\pi/4$.

## CONCLUSION

In this work, analytical solution for mechanical response of functionally graded cylinder under non-axisymmetric loads is presented. Modulus of elasticity varies along the thickness of the cylinder as a nonlinear function, but Poisson's ratio is considered invariant for the material. Internal pressures are periodically varying at inner surface of the cylinder along circumferential direction. The concept of Cauchy-Euler differential equation and Fourier half range series method are used to derive the results of mechanical stresses. The main advantage of this method is its applicability to any material model of functionally graded material. This method is better than the traditional potential function method as it does not have any mathematical limitation to handle general types of boundary conditions. This study may be useful in the application of pressure vessels.

## REFERENCES


1. Xu, C., Yu, Z.X., Du, F. (2019), *Dynamic analysis of a thick hollow cylinder made of two-dimensional functionally graded material using time-domain spectral element method*, Mech. Adv. Mater. Struct. 26(18): 1518-1535. doi: 10.1080/15376494.2018.1444224
2. Sobhani Aragh, B., Hedayati, H. (2012), *Static response and free vibration of two-dimensional functionally graded metal/ceramic open cylindrical shells under various boundary conditions*, Acta Mech. 223(2): 309-330. doi: 10.1007/s00707-011-0563-2
3. Evci, C., Gülgeç, M. (2018), Functionally graded hollow cylinder under pressure and thermal loading: Effect of material parameters on stress and temperature distributions, Int. J Eng. Sci. 123(C): 92-108. doi: 10.1016/j.ijengsci.2017.11.019
4. Jabbari, M., Sohrabpour, S., Eslami, M.R. (2003), *General solution for mechanical and thermal stresses in a functionally graded hollow cylinder due to nonaxisymmetric steady-state loads*, J. Appl. Mech. 70(1): 111-118. doi: 10.1115/1.1509484
5. Asgari, M., Akhlaghi, M., Hosseini, S.M. (2009), *Dynamic analysis of two-dimensional functionally graded thick hollow cylinder with finite length under impact loading*, Acta Mech. 208(3-4): 163. doi: 10.1007/s00707-008-0133-4
6. Nosrati, A.S., Parvizi, A., Afzal, S.A., Alimirzaloo, V. (2019), *Elasto-plastic solution for thick-walled spherical vessels with an inner FGM layer*, J Comput. Appl. Mech. 50(1): 1-13. doi: 10.22059/jcamech.2017.239277.173
7. Sahni, M., Sahni, R., Mehta, P. (2017), *Creep behaviour under $SiC_p$ exponential volume reinforcement in FGM composite rotating cylinders*, Mater. Today: Proceed. 4(9): 9529-9533. doi: 10.1016/j.matpr.2017.06.218
8. Sahni, M., Sahni, R. (2018), *Stress analysis of a pressurized functionally graded rotating discs with variable thickness and Poisson's ratio*, In: Gil-Lafuente A., Merigó J., Dass B., Verma R. (eds.) Applied Mathematics and Computational Intelligence, FIM 2015. Advances in Intelligent Systems and Computing, vol 730, Springer, Cham.: 54-62. doi: 10.1007/978-3-319-75792-6_5
9. Sahni, M., Sahni, R. (2018), *Elastic-plastic analysis for a functionally graded rotating cylinder under variation in Young's modulus*, In: Gil-Lafuente A., Merigó J., Dass B., Verma R. (eds.) Applied Mathematics and Computational Intelligence. FIM 2015. Advances in Intelligent Systems and Computing, Springer, Cham.: 26-39. doi: 10.1007/978-3-319-75792-6_3
10. Paul, S.K., Sahni, M. (2019), *Two-dimensional mechanical stresses for a pressurized cylinder made of functionally graded material*, Struct. Integ. and Life, 19(2): 79-85.
11. Singh, T.P., Sahni, M. (2016), *Study of strength of rotating discs of innovative composite material with variable thickness*, In: Proc. Int. MultiConference Eng. Comp. Scientists IMECS 2016, Vol. II, Hong Kong.
12. Yıldırım, V. (2017), *Exact thermal analysis of functionally graded cylindrical and spherical vessels*, Int. J Eng. Appl. Sci. 9(2): 112-126. doi: 10.24107/ijeas.318459
13. Fesharaki, J.J., Roghani, M. (2020), *Thermo-mechanical behavior of a functionally graded hollow cylinder with an elliptic hole*, J Braz. Soc. Mech. Sci. Eng. 42(1): 66. doi: 10.1007/s40430-019-2135-7
14. Delouei, A.A., Emamian, A., Karimnejad, S., et al. (2019), *On 2D asymmetric heat conduction in functionally graded cylindrical segments: A general exact solution*, Int. J Heat Mass Trans. 143: 118515. doi: 10.1016/J.IJHEATMASSTRANSFER.2019.118515
15. Yadav, A., Amabili, M., Panda, S.K., Dey, T. (2019), *Nonlinear vibration response of functionally graded circular cylindrical shells subjected to thermo-mechanical loading*, Compos. Struct. 229: 111430. doi: 10.1016/j.compstruct.2019.111430
16. Sofiyev, A.H., Dikmen, F. (2021), *Buckling analysis of functionally graded shells under mixed boundary conditions subjected to uniform lateral pressure*, J Appl. Comput. Mech. 7(1): 345-354. doi: 10.22055/jacm.2020.35564.2684
17. Shao, Z.S., Wang, T.J., Ang, K.K. (2007), *Transient thermo-mechanical analysis of functionally graded hollow circular cylinders*, J Thermal Stresses 30(1): 81-104. doi: 10.1080/01495730600897211
18. Jabbari, M., Nejad, M.Z., Ghannad, M. (2015), *Thermo-elastic analysis of axially functionally graded rotating thick cylindrical pressure vessels with variable thickness under mechanical loading*, Int. J Eng. Sci. 96: 1-18. doi: 10.1016/j.ijengsci.2015.07.005
19. Bayat, M., Sahari, B.B., Saleem, M., et al. (2009), *Thermo elastic analysis of functionally graded rotating disks with temperature-dependent material properties: uniform and variable thickness*, Int. J Mech. Mater. Des. 5(3): 263-279. doi: 10.1007/s10999-009-9100-z
20. Tutuncu, N. (2007), *Stresses in thick-walled FGM cylinders with exponentially-varying properties*, Eng. Struct. 29(9): 2032-2035. doi: 10.1016/j.engstruct.2006.12.003
21. Yas, M.H., Sobhani Aragh, B. (2010), *Three-dimensional analysis for thermoelastic response of functionally graded fiber reinforced cylindrical panel*, Compos. Struct. 92(10): 2391-2399. doi: 10.1016/j.compstruct.2010.03.008
22. Poultangari, R., Jabbari, M., Eslami, M.R. (2008), *Functionally graded hollow spheres under non-axisymmetric thermo-mechanical loads*, Int. J Pres. Ves. Piping, 85(5): 295-305. doi: 10.1016/j.ijpvp.2008.01.002
23. Mahbadi, H. (2017), *Stress intensity factor of radial cracks in isotropic functionally graded solid cylinders*, Eng. Fract. Mech. 180: 115-131. doi: 10.1016/j.engfracmech.2017.05.019
24. Kayhani, M.H., Norouzi, M., Delouei, A.A. (2012), *A general analytical solution for heat conduction in cylindrical multilayer composite laminates*, Int. J Therm. Sci. 52: 73-82. doi: 10.1016/J.IJTHERMALSCI.2011.09.002
25. Kamdi, D.B., Lamba, N.K. (2016), *Thermoelastic analysis of functionally graded hollow cylinder subjected to uniform temper-*

*ature field*, J Appl. Comput. Mech. 2(2): 118-127. doi: 10.22055/jacm.2016.12414
26. Akbaş, Ş.D. (2017), *Vibration and static analysis of functionally graded porous plates*, J Appl. Comput. Mech. 3(3): 199-207. doi: 10.22055/jacm.2017.21540.1107
27. Le, N.L., Nguyen, T.P., Vu, H.N., et al. (2020), *An analytical approach of nonlinear thermo-mechanical buckling of functionally graded graphene-reinforced composite laminated cylindrical shells under compressive axial load surrounded by elastic foundation*, J Appl. Comput. Mech. 6(2): 357-372. doi: 10.22055/jacm.2019.29527.1609
28. Delouei, A.A., Emamian, A., Karimnejad, S., Sajjadi, H. (2019), *A closed-form solution for axisymmetric conduction in a finite functionally graded cylinder*, Int. Comm. Heat Mass Transfer, 108: 104280. doi: 10.1016/j.icheatmasstransfer.2019.104280
29. Yarimpabuç, D. (2020), *Nonlinear thermal stress analysis of functionally graded thick cylinders and spheres*, Iran. J Sci. Technol. Trans. Mech. Eng. Oct: 1-9. doi: 10.1007/s40997-020-00395-0
30. Benslimane, A., Benchallal, R., Mammeri, S., et al. (2021), *Investigation of displacements and stresses in thick-walled FGM cylinder subjected to thermo-mechanical loadings*, Int. J Comput. Meth. Eng. Sci. Mech. 22(2): 138-149. doi: 10.1080/15502287.2020.1853853
31. Enab, T.A. (2014), *Stress concentration analysis in functionally graded plates with elliptic holes under biaxial loadings*, Ain Shams Eng. J, 5(3): 839-850. doi: 10.1016/j.asej.2014.03.002



## ESIS Special Issues 2019-2020

| Journal | Title | Source | Editor | Status |
|---|---|---|---|---|
| International Journal of Fatigue | Fatigue crack paths 2018 | Crack path 2018 | A. Carpinteri, F. Berto, Y. Hong, Th. Palin-Luc | IJF 121-125, April-November 2019 |
| Theoretical and Applied Fracture Mechanics | Crack Paths 2018 | Crack path 2018 | A.Carpinteri, F. Iacoviello, L. Pook, S. Vantadori | TAFM, 2019 (virtual Special Issue) |
| Engineering Failure Analysis | 2nd International Conference on Structural Integrity and Durability | ICSID 2018 | Ž. Božić, R. Clegg, L. Banks-Sills, F. Berto, F. Iacoviello | EFA, 2019 (virtual Special Issue) |
| Engineering Failure Analysis | ECF22 2018 | ECF22 | | EFA, 2019 (virtual Special Issue) |
| Engineering Failure Analysis | ISRAS-TC12 | International Symposium on Risk analysis and Safety of Large Structures and Components | J.A. Correia, A. Sedmak, V. Moskvichev, A. Jesus, M. Muñiz-Calvente | EFA, 2019 (virtual Special Issue) |
| Theoretical and Applied Fracture Mechanics | Multiaxial Fracture 2019 | The 12th International Conference on Multiaxial Fatigue and Fracture | Th. Palin-Luc, A. Carpinteri, M. Endo, F. Morel, M. Vormwald | TAFM, 2020 (virtual Special Issue) |
| Engineering Failure Analysis | ISRAS-TC12 | International Symposium on Risk analysis and Safety of Large Structures and Components (TC12/ESIS) | J.A. Correia, M. Muñiz-Calvente, A. Jesus, A. Sedmak, V. Moskvichev, R. Calçada | EFA, 2020 (virtual Special Issue) |
| Engineering Failure Analysis | ICSI 2019 | International Conference on Structural Integrity 2019 | V. Infante, P. Moreira, P. Tavares | EFA, 2020 (virtual Special Issue) |
| International Journal of Fatigue | Multiaxial Fatigue 2019 | The 12th International Conference on Multiaxial Fatigue and Fracture (ICMFF12) | A. Carpinteri, F. Dunne, A. Fatemi, F. Morel, Th. Palin-Luc | IJF, 2020 (virtual Special Issue) |
| International Journal of Fatigue | ECF22 | 22nd European Conference on Fracture (ECF 22) | A. Sedmak, F. Iacoviello, V. Silberschmidt, S. Schmauder | IJF, 2020 (virtual Special Issue) |
| Theoretical and Applied Fracture Mechanics | Special issue ESIAM19 Theoretical and Applied Fracture Mechanics | The First European Conference on Structural Integrity of Additively Manufactured Materials | F. Berto, J. Torgersen, M. Benedetti, S. Bagherifard, Ch. Bo, G. Qian | TAFM, 2020 (virtual Special Issue) |